

EIGHT NEW MILLISECOND PULSARS IN NGC 6440 AND NGC 6441

PAULO C. C. FREIRE¹, SCOTT M. RANSOM², STEVE BÉGIN^{3, 4}, INGRID H. STAIRS³, JASON W. T. HESSELS⁵, LUCILLE H. FREY⁶, AND FERNANDO CAMILO⁷

Draft version October 22, 2018

ABSTRACT

Motivated by the recent discovery of 30 new millisecond pulsars in Terzan 5, made using the Green Bank Telescope’s S-band receiver and the Pulsar Spigot spectrometer, we have set out to use the same observing system in a systematic search for pulsars in other globular clusters. Here we report on the discovery of five new pulsars in NGC 6440 and three in NGC 6441; each cluster previously had one known pulsar. Using the most recent distance estimates to these clusters, we conclude that there are as many potentially observable pulsars in NGC 6440 and NGC 6441 as in Terzan 5. We present timing solutions for all of the pulsars in these globular clusters. Four of the new discoveries are in binary systems; one of them, PSR J1748–2021B (NGC 6440B), has a wide ($P_b = 20.5$ d) and eccentric ($e = 0.57$) orbit. This allowed a measurement of its rate of advance of periastron, $\dot{\omega} = 0.00391(18)^\circ\text{yr}^{-1}$. If due to the effects of general relativity, the total mass of this binary system is $2.92 \pm 0.20 M_\odot$ (1σ), implying a median pulsar mass of $2.74 \pm 0.21 M_\odot$. There is a 1% probability that the inclination is low enough that pulsar mass is below $2 M_\odot$, and 0.10% probability that it is between 1.20 and $1.44 M_\odot$. If confirmed, this anomalously large mass would strongly constrain the equation of state for dense matter. The other highly eccentric binary, PSR J1750–37A, has $e = 0.71$, and $\dot{\omega} = 0.0055(3)^\circ\text{yr}^{-1}$, implying a total system mass of $1.97 \pm 0.15 M_\odot$ and, along with the mass function, maximum and median pulsar masses of 1.65 and $1.26 M_\odot$ respectively.

Subject headings: binaries: general — stars: neutron — pulsars: general — globular clusters: individual (NGC 6440, NGC 6441) — equation of state

1. INTRODUCTION

A recent survey of the globular cluster (GC) Terzan 5 with the S-band (1.7 to 2.6 GHz) receiver of the Green Bank Telescope (GBT) and the Pulsar Spigot spectrometer (Kaplan et al. 2005) has met with extraordinary success, finding 30 new millisecond pulsars (MSPs). The first 21 discoveries were announced in Ransom et al. (2005). More recently, nine more pulsars were discovered⁸, including PSR J1748–2446ad, the fastest spinning pulsar known (Hessels et al. 2006). These discoveries show that this observing system (henceforth GBT/S/PS) has an unprecedented sensitivity to MSPs outside the Arecibo sky, due in great part to the factor of 3 higher gain of the GBT as compared to the Parkes telescope. Perhaps even more importantly, the higher observing frequency (~ 2 GHz), large observing bandwidth (600 MHz), and relatively fine frequency resolution (~ 0.78 MHz) retain high sensitivity and time resolution for MSPs with large dispersion measures (DM). The discovery of the 1.39 ms PSR J1748–2446ad at a

DM of $235.6 \text{ cm}^{-3}\text{pc}$ dramatically demonstrates the sensitivity of the GBT/S/PS system to fast-spinning pulsars at high DMs. This motivated us to search for MSPs in other promising GCs with the GBT/S/PS system.

1.1. Cluster selection

In the high stellar density environments in the cores of GCs, binary systems with at least one main sequence (MS) star are occasionally disrupted by the intrusion of a neutron star (NS). The most likely outcome is an “exchange encounter”, where the lightest component of the previous binary is ejected and a NS-MS binary remains. The resulting NS-MS systems can become much more numerous than those formed from evolution of primordial binaries. With the evolution of the MS star, it can happen that matter will accrete onto the NS during a Low-Mass X-ray Binary (LMXB) phase, particularly among the more compact systems. When the LMXB accretion stops, we are left with an MSP orbiting a white dwarf (WD) star.

Pooley et al. (2003) showed a strong correlation between the number of X-ray point sources in a GC (which are generally compact binaries) and the rate of stellar encounters within the half-mass radius, a parameter that they designate Γ . This correlation is stronger than for any other individual GC parameter, and applies to active LMXBs as well (although with only a dozen systems in the Galactic GC system, the statistics are poorer). Γ might therefore be a good indicator of the present rate of MSP formation. Pooley et al. (2003) provide a simple way of calculating the stellar interaction rate at the core of any GC:

$$\Gamma_c \propto \rho_0^{1.5} r_c^2, \quad (1)$$

¹ National Astronomy and Ionosphere Center, Arecibo Observatory, PR 00612; pfreire@naic.edu

² National Radio Astronomy Observatory, Charlottesville, VA 22903

³ Department of Physics and Astronomy, University of British Columbia, Vancouver, BC V6T 1Z1, Canada

⁴ Département de physique, de génie physique et d’optique, Université Laval, Québec, QC G1K 7P4, Canada

⁵ “Astronomical Institute ”Anton Pannekoek”, University of Amsterdam, Kruislaan 403, 1098 SJ Amsterdam, The Netherlands

⁶ Department of Astronomy, Case Western Reserve University, Cleveland, OH 44106

⁷ Columbia Astrophysics Laboratory, Columbia University, New York, NY 10027

⁸ See [http://www2.naic.edu/~sim\\$pfreire/GCpsr.html](http://www2.naic.edu/~sim$pfreire/GCpsr.html)

TABLE 1
THE SIX GLOBULAR CLUSTERS WITH HIGHEST Γ_c

Globular Cluster	D^a (kpc)	ρ_0^b ($\log [L_\odot \text{pc}^{-3}]$)	Γ_c (%)	DM ^c (cm^{-3}pc)	$\tau_{\text{scatt},2\text{GHz}}^d$ (μs)	N_{psr}^e	ΔT^f (hr)	DM Ref. ^g
NGC 6388	10.0	5.34	9.5	318	1.4	0	2.2	
Terzan 5	10.3	5.06	8.6	(234.3–245.6)	6	3 + 30	8.0	(1)
NGC 6441	11.7	5.25	8.0	(230.1–234.4)	2	1 + 3	5.3	(2)
NGC 6440	8.4	5.28	6.4	(219.4–227.0)	5	1 + 5	8.4	(3)
NGC 6266	6.9	5.14	5.1	(113.4–115.0)	4	6	7.0	(4)
Liller 1	9.6	5.53	4.2	771	$\sim 3 \times 10^2$	0	6.2	

^a Distance from the Solar System from Harris (1996). These values have significant systematic uncertainties.

^b Central density of GC; see last column of third table in [http://physwww.mcmaster.ca/~sim\\$harris/mwgc.dat](http://physwww.mcmaster.ca/~sim$harris/mwgc.dat).

^c For GCs with known pulsars, we present the DM range for the known pulsars, with references in the last column, otherwise we predict the DM for the GC's estimated distance using the Cordes & Lazio (2001) model. These can be off by a factor of up to about 2.

^d Extrapolated from other frequencies using $\tau_{\text{scatt},2\text{GHz}} = \tau_{\text{scatt}}(F)(F/2\text{GHz})^{4.4}$. In the case of Terzan 5, the scattering was measured by Nice & Thorsett (1992) as $700 \mu\text{s}$ at 685 MHz. Otherwise, we scale the scattering time at 1GHz predicted by the Cordes & Lazio (2001) model for the DM in the previous column. These can be off by up to an order of magnitude.

^e Number of previously known pulsars + **number of new pulsars**.

^f Amount of time the GC is visible at the GBT per day

^g (1) Ransom et al. 2005, (2) Possenti et al. 2006, this work, (3) Lyne, Manchester & D'Amico 1996, this work, (4) Possenti et al. 2003, Chandler 2003.

TABLE 2
PARAMETERS FOR THREE GLOBULAR CLUSTERS

	NGC 6388	NGC 6440	NGC 6441
Right Ascension of center, α	17 ^h 36 ^m 17 ^s .0	17 ^h 48 ^m 52 ^s .7	17 ^h 50 ^m 12 ^s .9
Declination of center, δ	−44°44′06″	−20°21′37″	−37°03′05″
Galactic longitude, l (°)	345.56	7.73	353.53
Galactic latitude, b (°)	−6.74	3.80	−5.01
Cluster distance, D (kpc)	10.0	8.2 ^a	13.5 ^a
Angular core radius, θ_c (arcmin)	0.12	0.13	0.11
Half-mass radius, θ_h (arcmin)	0.67	0.58	0.64
Metallicity ($\log[\text{Fe}/\text{H}]$)	−0.60	−0.34	−0.53
$v_z(0)$ (km s^{-1})	19.13 ^b	13.01 ^b	19.5 ^{+9.4c} _{−5.1}
a_G^d (10^{-9}m s^{-2})	−0.46	−0.029	−0.46

NOTE. — Parameters as in Harris (1996), except where indicated.

^a Valenti et al. (2007).

^b Webbink (1985).

^c Dubath et al. (1997).

^d Calculated using the data above and the Kuijken & Gilmore (1989) model of the Galaxy.

where ρ_0 is the central mass density and r_c is the core radius. This parameter is perhaps more relevant than Γ for the formation of LMXBs because mass segregation constrains neutron stars to within a few core radii of the center of the GC.

We calculated Γ_c for all Galactic GCs with the central luminosity densities and core radii given in Harris (1996)⁹, and assuming a constant conversion factor between central luminosity density and central mass density. The six best GCs are listed in Table 1, with their Γ_c presented as a percentage of the total Γ_c summed over all Galactic GCs. This table represents our initial survey expectations; we hypothesized that the percentages should be closely related to the fraction of the total GC MSP population contained in each GC.

For the first phase of the survey, we selected the GCs

⁹ See <http://physwww.mcmaster.ca/~harris/mwgc.dat> for an updated list of GC parameters.

in Table 1 that had not been previously searched with the GBT/S/PS system: NGC 6388, NGC 6440 and NGC 6441. Liller 1 was searched at the same time as Terzan 5 by Ransom et al. (2005) and NGC 6266 has been searched by Jacoby et al. (2002). Despite the large predicted stellar interaction rates, only two pulsars were known in these GCs: PSR B1745–20A (NGC 6440A; Lyne et al. 1996) and PSR J1750–37A (NGC 6441A; Possenti et al. 2006). The spin periods and DMs of NGC 6440A and NGC 6441A are 288.6 ms and 111.6 ms and 220 and 234 cm^{-3}pc , respectively. We assumed that the lack of other known pulsars in these high-DM GCs was largely due to a bias of the earlier surveys against the detection of faster-spinning MSPs. The high central frequency and improved time resolution of the GBT/S/PS system greatly diminish pulse broadening due to multipath propagation and dispersive smearing, and would therefore alleviate the bias against the detection of other MSPs in these GCs.

1.2. Data taking

From 2005 April 18 to August 21, we observed NGC 6388, NGC 6440 and NGC 6441 on three different occasions each, using the GBT's S-band receiver with the Pulsar Spigot. The longest integration times used for each GC are very close to their maximum track times indicated in Table 2.

These observations take advantage of the relatively radio-frequency-interference (RFI) clean band between 1650 and 2250 MHz. The Pulsar Spigot is built around the GBT correlation spectrometer and is available in a number of modes (Kaplan et al. 2005). For most observations, we used the Spigot in mode 2 where two orthogonal polarizations with a total bandwidth of 800 MHz are digitized with three levels, autocorrelated with 1024 lags, and integrated for 81.92 μ s. The resulting autocorrelation functions are summed and then written to disk as 16-bit integers. After Fourier transforming the lags, we have 768 usable channels across the 600-MHz bandpass (0.78125-MHz channels). At a frequency of 2 GHz and a DM of 220 cm^{-3} pc, the dispersive smearing across one channel is 178 μ s. Recently, we have been using mode 14, this mode writes the 81.92- μ s integrations to disk as 8-bit integers, but with twice the frequency resolution, resulting in a dispersive smearing across one channel for a DM of 220 cm^{-3} pc of 89 μ s.

In the case of NGC 6440 and NGC 6441, the discovery of new pulsars lead us to observe these two GCs on a total of 37 and 24 extra occasions respectively, from 2005 November 5 to 2007 March 28 (Spigot mode 2), and then from 2007 October 10 to November 1 (Spigot mode 14), the latter data has only been added to the ephemeris of NGC 6440B (see §3). The typical observing session spends the first 2-3 hours on NGC 6440, then observes NGC 6441 for 2.5 to 4 hours, and then spends 2 to 3 hours again on NGC 6440. The total usable observing times are about 90–100 hr for each pulsar in NGC 6440 and NGC 6441.

On two occasions, we observed NGC 6440 and NGC 6441 at 820 MHz with a bandwidth of 50 MHz in order to determine the DMs of the pulsars more accurately and to search for pulsars with spectral indices too steep to be detected at 1950 MHz, or that lie outside the area covered by the S-band beam. Because the telescope beam widths at these frequencies (6'5 at 1.95 GHz and 15' at 820 MHz) are significantly larger than the half-mass radii of these GCs (see Table 2), we observed only single positions centered on the GCs.

2. SEARCH AND DISCOVERY OF NEW PULSARS

After masking the interference (in the manner described in detail in Hessels et al. 2007), the search data (taken in Spigot mode 2) were dedispersed in 48 sub-bands over the whole 600-MHz usable band at the “average” DMs for NGC 6440 (223 cm^{-3} pc) and NGC 6441 (233 cm^{-3} pc), reducing the volume of data to be stored by a factor of ~ 20 . For each sub-band set we created ~ 40 dedispersed time series covering a range of trial DMs $\pm 10 \text{ cm}^{-3}$ pc around the nominal GC DMs in steps of 0.5 cm^{-3} pc. If a pulsar has a DM halfway between two trial DMs, that introduces an extra smearing of 168 μ s, resulting in a total maximum smearing of 245 μ s. We

also barycentered each time series using TEMPO¹⁰.

We Fourier transformed each time series and searched them using a frequency domain acceleration search technique (Ransom et al. 2002) that allows a fully coherent search in frequency/frequency-derivative space as well as the incoherent addition of a number of harmonics (1, 2, 4, 8 or 16). The technique has an optimal sensitivity for pulsars in binary systems with an orbital period much longer than the observation time ($P_{\text{orb}} \geq 10T_{\text{obs}}$). For this reason, the acceleration searches were performed on all the observations for the entire length of each observation as well as on overlapping segments of various shorter durations (typically 27 and 82 minutes). A more detailed description of the search procedure is presented in Hessels et al. (2007).

We discovered eight new MSPs, all in S-band data, five of them in NGC 6440 and three in NGC 6441. Preliminary results on these objects were presented in Bégin (2006). Their pulse profiles, together with those of the previously known objects, are presented in Figure 1. These pulse profiles were obtained by adding *all* detections of the pulsars made in mode 2, carefully excluding all sub-integrations in time or frequency that are corrupted by significant RFI.

We found no pulsars in NGC 6388, possibly due to dispersive smearing and/or interstellar scattering being substantially higher than the prediction given in Table 1. The search for pulsars in NGC 6388 was further hindered by the small time the GBT can observe the GC (2.2 hrs; see Table 1). Furthermore, many of the pulsars in Terzan 5, NGC 6440 and NGC 6441 were found by searching follow-up timing observations, none of which were made for NGC 6388.

2.1. Flux densities

The 1950 MHz flux densities (S_{1950}) of all the pulsars in NGC 6440 and NGC 6441 and their pseudo-luminosities at the same frequency ($L_{1950} \equiv S_{1950}D^2$) are listed in Tables 3 (isolated pulsars) and 4 (binary pulsars). These were determined from the pulse profiles in Fig. 1 by assuming that the off-pulse r.m.s. is as predicted by the radiometer equation for the total observing time. In calculating the system's equivalent flux density, we used a system temperature of 26K towards NGC 6440 and 28 K towards NGC 6441, a gain of 1.95 K/Jy for the GBT at S-band and multiplied the result by 1.235 for the 3-level efficiency factor of the correlator.

These flux densities indicate that some of the new discoveries, particularly in NGC 6441, are as faint as the faintest pulsars in Terzan 5, suggesting that we have reached a similar sensitivity in our survey as in that reported by Ransom et al. (2005).

We can compare the sizes of the pulsar populations in these clusters with that of Terzan 5 by comparing the distribution of their pseudo-luminosities. The observing system and observing frequency are the same, the DMs of the pulsars are very similar, the scattering times are similarly small, the length of the integrations are similar (Table 1) and the search software is the same, making the search similarly sensitive to fast-spinning pulsars (§2.2). Furthermore, the software used to make the flux density measurements is similar (but not exactly - some refine-

¹⁰ <http://www.atnf.csiro.au/research/pulsar/tempo/>

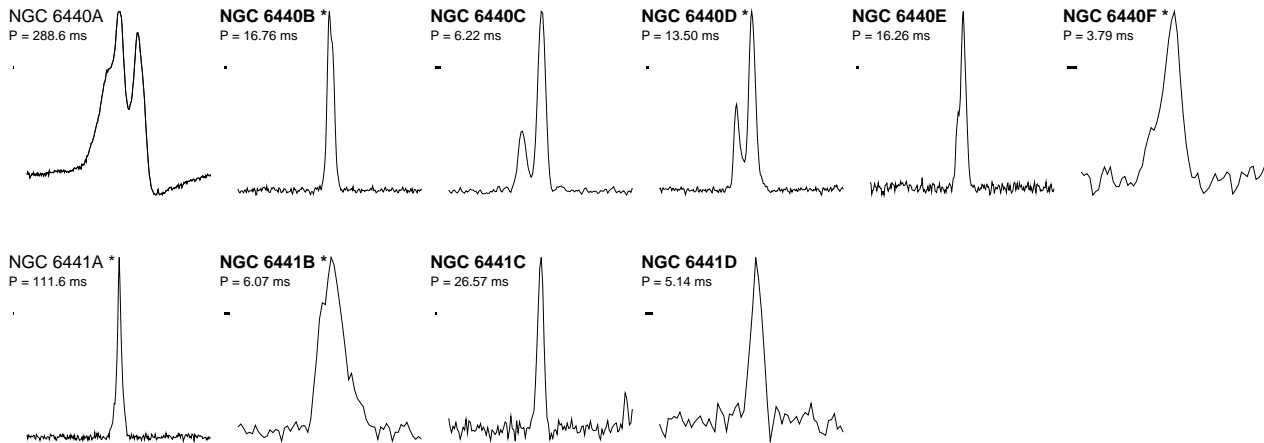


FIG. 1.— Average 1950 MHz pulse profiles for the 10 pulsars known in the GCs NGC 6440 and NGC 6441, obtained by adding all observations made with mode 2 of the Pulsar Spigot. These profiles cover one full rotation. The pulsars in binary systems have an asterisk after their names, and the newly discovered pulsars have their names in boldface. The horizontal width of the rectangles indicates the system’s total time resolution in mode 2, including the effects of dispersive smearing, relative to each pulsar’s spin period. The dip in power after the main pulse of NGC 6440A is likely a Spigot artifact.

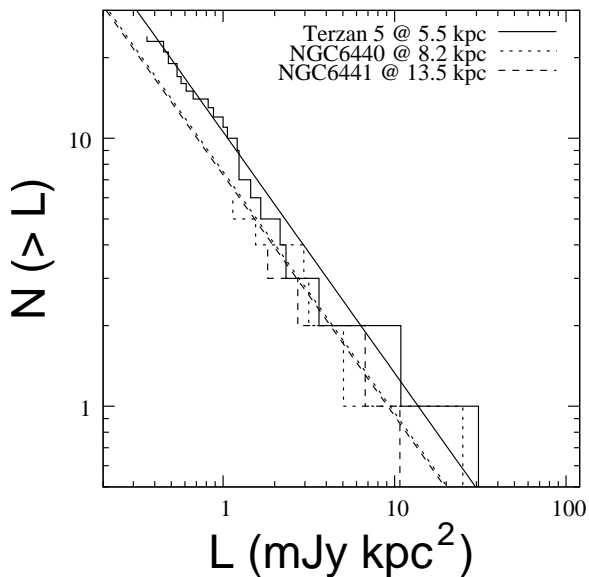


FIG. 2.— Cumulative distribution of pseudo-luminosities at 1950 MHz for the pulsars in NGC 6440, NGC 6441 and Terzan 5. The pseudo-luminosities are estimated assuming the most recent GC distance estimates (Ortolani et al. 2007, Valenti et al. 2007).

ments have recently been added to the program). All these factors make the flux densities directly comparable; the pseudo-luminosities will then be directly comparable as well if the GC distances are accurate.

We have fitted a luminosity function of the type $N(>L) = k_1 L^{-0.9}$ (derived by Hessels et al. 2007 as a best fit to the luminosities of 41 isolated pulsars in M5, M13, M15, M28, Terzan 5, 47 Tucanae, NGC 6440 and NGC 6441 above $L_{1400} = 1.5$ mJy kpc²), where $N(>L)$ is the number of pulsars above a pseudo-luminosity of L and k_1 is the number of pulsars brighter than 1 mJy kpc². If we assume the distances listed in Harris (1996, see Table 1), we obtain $k_1 = 32.8, 7.9$ and 5.7 for Terzan 5, NGC 6440 and NGC 6441 respectively. This would indicate that Γ_c does a poor job at predicting the number of MSPs in these GCs.

However, recent studies of these GCs have changed these distance estimates (see Table 2), sometimes drastically: in the case of Terzan 5, the most recent distance estimate is 5.5 kpc (Ortolani et al. 2007). It should be noted that these new distance estimates still have large systematic uncertainties (Heinke and Ortolani, private communication). These values affect our prediction for Γ_c : the total absolute visible luminosity of the core of the GC is proportional to D^2 , but the volume of the core is proportional to D^3 , therefore $\rho_0 \propto D^2/D^3 = D^{-1}$. Inserting this in Eq. 1, and keeping in mind that r_c is also proportional to D , we obtain $\Gamma_c \propto D^{1/2}$. With the revised distance estimates, we obtain revised Γ_c values of 6.3, 6.3 and 8.6% for Terzan 5, NGC 6440 and NGC 6441 respectively.

When we use the new distance estimates to re-calculate the pseudo-luminosities of the pulsars in these three GCs (Fig. 2), we obtain $k_1 = 10.6, 7.5$ and 7.3 for Terzan 5, NGC 6440 and NGC 6441 respectively. Given the uncertainties in the distance estimates, this is consistent with all the clusters having similarly sized pulsar populations, and Γ_c being a good predictor of the number of pulsars in a GC.

If the k_1 numbers reflect the sizes of the pulsar populations, then assuming the Hessels et al. (2007) luminosity law, we should detect

$$N_{\text{PSR,NGC6440}} = N_{\text{PSR,Ter5}} (k_{1,\text{NGC6440}}/k_{1,\text{Ter5}}) (D_{\text{Ter5}}^2/D_{\text{NGC6440}}^2)^{0.9} \quad (2)$$

pulsars in NGC 6440 and 4.1 pulsars for NGC 6441¹¹. For NGC 6441, we detect as many pulsars as expected from the luminosity distribution given its greater distance, but we don’t detect faint (10 - 17 μ Jy) pulsars in NGC 6440. This could happen if some of them are in tight binary systems, which would make them more difficult to detect. In any case, the most likely reason why we detect more pulsars in Terzan 5 is simply because that GC is closer to us.

To summarize, we can see from the discussion above

¹¹ The number of pulsars in Terzan 5 we use in this calculation is 30. This many were detected using the same search methods employed in the present survey.

that the distance to the GC does not have a major impact on the estimate of Γ_c ($\Gamma_c \propto D^{1/2}$), but it has a fundamental impact in estimating pulsar populations from the observed flux densities ($k_1 \propto D^{2 \times 0.9}$). For Terzan 5, NGC 6440 and NGC 6441, the use of the latest distance estimates makes Γ_c a good predictor of the relative sizes of the pulsar populations.

2.2. Spin period distribution

Looking at the spin periods in Table 6, and comparing them with the spin periods of the pulsars in other GCs¹², we notice a conspicuous absence of fast-spinning objects. Of the 33 known pulsars in Terzan 5 (a GC for which the discovery observations have very nearly the same time resolution as in our survey), 15 have spin periods shorter than that of NGC 6440F, the fastest MSP we found, and 23 have spin periods shorter than that of NGC 6441D.

This could be a result of interstellar scattering being worse for NGC 6440 and NGC 6441 than it is for Terzan 5. Looking at Table 1, we can see that both NGC 6440 and NGC 6441 have predicted scattering times *lower* than those of Terzan 5. An inspection of the pulse profiles in Figure 1, particularly of the shorter-period pulsars such as NGC 6440C and NGC 6441D, does not reveal the typical signature of interstellar scattering, an exponential decay of intensity after the main peak, as one would expect from the small scattering timescales in Table 1. The difference, if statistically significant, is likely to be real, not due to scattering or dispersive smearing.

A two-sided Kolmogorov-Smirnov (2K-S) test (Press et al. 1992) gives an 87% probability that the spin period distributions NGC 6440 and NGC 6441 are those of a common population. Comparing these two with Terzan 5, we obtain, respectively, 1.1% and 1.8% probabilities for the same hypothesis. Comparing these two with the pulsar population in 47 Tucanae, we obtain probabilities of 0.13% and 0.27% respectively.

This phenomenon is not restricted to NGC 6440 and NGC 6441. A recent 1.4 GHz GC pulsar survey made with the Arecibo telescope (Hessels et al. 2007) has searched for pulsars in M15. Despite being even more sensitive to short-period pulsars than the Terzan 5 survey, it found none. The spin period distribution of the M15 pulsars detected by Hessels (2007) is indistinguishable from those of NGC 6440 and NGC 6441 (2K-S probabilities of 62% and 65%), but different from that of Terzan 5 (2K-S probability of 2.6%).

2.3. Dispersion measure distribution

The DMs of the known pulsars in NGC 6440 range from 219.4 to 226.9 $\text{cm}^{-3} \text{pc}$, a span of 7.5 $\text{cm}^{-3} \text{pc}$. In Terzan 5, the known pulsars have DMs between 234.3 to 243.5 $\text{cm}^{-3} \text{pc}$, a span of 9.2 $\text{cm}^{-3} \text{pc}$ (Ransom et al. 2005). However, two of the pulsars in Terzan 5 (A and D) have anomalously high DMs. Each of these pulsars is spatially more distant from the center of the GC than the other pulsars. All the other pulsars have DMs between 234.32 and 239.82 $\text{cm}^{-3} \text{pc}$. If we randomly choose six pulsars in Terzan 5, there is a 66% probability that the set will include none of the two outliers. In that case, the maximum DM span will be

5.5 $\text{cm}^{-3} \text{pc}$, lower than but comparable to what we observe in NGC 6440.

This is consistent with the idea that the variations in DM between pulsars are generally due to differences in the Galactic electron column density¹³. Since both NGC 6440 and Terzan 5 are at similar DMs, and have their pulsars spread over roughly similar areas of the sky, the differences in DM between the pulsars should be similar. The spread in DMs seems to be linearly correlated with the absolute DM of the GC (Freire et al. 2005), an idea which is supported by the observed spread of DMs in NGC 6440.

For NGC 6441, where only four pulsars are known, the DMs range between 230.09 and 234.39 $\text{cm}^{-3} \text{pc}$. The slightly more compact distribution of the smaller number of pulsars is likely to produce a smaller range of DMs than observed in NGC 6440.

3. TIMING

Diffraction scintillation causes a modulation of the intensity of the pulsed signal in time and frequency. “Scintles” are the regions of the dynamic spectrum where the signal is amplified relative to average. The high DMs of these pulsars imply that the scintles have narrow bandwidths (of the order of ~ 20 kHz and ~ 60 kHz at 1.95 GHz for NGC 6440 and NGC 6441, Cordes and Lazio 2001), and are therefore averaged out over our wide observing band. This means that the flux densities of the pulsars are very steady, resulting in the very high detection rate during our timing campaign: even the faintest new MSPs are always detectable. These detections were cross-correlated with a synthetic profile, obtained from fitting a minimal set of Gaussian curves to the summed profiles presented in Figure 1. This cross-correlation is done in the Fourier domain, as described in Taylor (1992), and from it we derive pulse times of arrival (TOAs). For the faint, isolated pulsars we calculated about 1 TOA per observation, but for the binary systems, like NGC 6440B and particularly NGC 6440D, a significantly larger number were calculated in order to retain orbital phase information.

These TOAs were fitted to a pulsar model containing spin (its frequency ν and its first derivative $\dot{\nu}$) and astrometric (right ascension α and declination δ) parameters, plus the DM using TEMPO. The parameters obtained from these fits are presented in Tables 3 and 4. To account for the motion of the telescope relative to the barycenter of the solar system, we used the DE405 Solar System ephemeris (Standish 1998). The DMs are calculated by comparing pulse TOAs at 820 and 1950 MHz, but they assume that there is no significant longitudinal evolution of the pulse profile with frequency. For the binary pulsars, the orbital parameters (orbital period P_b ; semi-major axis of the pulsar’s orbit a projected along the line-of-sight in light-seconds, $x \equiv a \sin i/c$; eccentricity e ; longitude of periastron ω ; time of passage through periastron T_0 ; and in two cases the rate of advance of periastron $\dot{\omega}$) were also fitted (see Table 4) using the the Damour & Deruelle orbital model (Damour & Deruelle 1985;

¹³ The exception is 47 Tucanae (Freire et al. 2001), where the DM differences between pulsars are predominantly due to gas intrinsic to the GC.

¹² See <http://www.naic.edu/~pfreire/GCpsr.html>.

TABLE 3
PARAMETERS FOR THE ISOLATED PULSARS IN NGC 6440 AND NGC 6441

	PSR B1745–20A (NGC 6440A)	PSR J1748–2021C (NGC 6440C)	PSR J1748–2021E (NGC 6440E)	PSR J1750–3703C (NGC 6441C)	PSR J1750–3703D (NGC 6441D)
Observation and data reduction parameters					
S_{1950}^a (mJy)	0.37	0.044	0.023	0.015	0.010
L_{1950}^b (mJy kpc ²)	25	3.0	1.5	2.7	1.8
Number of TOAs	107	161	61	82	68
Residual rms (μ s)	452	38	21	100	53
EFAC	1.72	3.37	1.02	1.17	1.25
Reference Epoch (MJD)	54000	54000	54000	54000	54000
Timing parameters					
α (J2000)	17 ^h 48 ^m 52 ^s .689(2)	17 ^h 48 ^m 51 ^s .17320(15)	17 ^h 48 ^m 52 ^s .80040(14)	17 ^h 50 ^m 13 ^s .4541(7)	17 ^h 50 ^m 13 ^s .0969(4)
δ (J2000)	–20°21′39″.7(5)	–20°21′53″.81(4)	–20°21′29″.38(3)	–37°03′05″.58(3)	–37°03′06″.368(17)
ν (Hz)	3.464969947246(19)	160.59270990836(6)	61.48547652886(2)	37.63830424257(6)	194.55492232569(15)
$\dot{\nu}$ (10 ^{–15} Hz s ^{–1})	–4.7944(12)	1.543(4)	–1.1812(15)	1.411(4)	–18.652(9)
DM (cm ^{–3} pc)	219.4(2)	226.95(6)	224.10(4)	230.67(2)	230.09(17)

^a The uncertainties in these fluxes are of the order of 10%.

^b In this and the next table, the distances used to calculate this parameter are those given in Table 2

TABLE 4
PARAMETERS FOR THE BINARY PULSARS IN NGC 6440 AND NGC 6441

	PSR J1748–2021B (NGC 6440B)	PSR J1748–2021D (NGC 6440D)	PSR J1748–2021F (NGC 6440F)	PSR J1750–37A (NGC 6441A)	PSR J1750–3703B (NGC 6441B)
Observation and data reduction parameters					
S_{1950} (mJy)	0.047	0.075	0.017	0.059	0.037
L_{1950} (mJy kpc ²)	3.2	5.0	1.1	10.8	6.7
Number of TOAs	1051	946	52	129	277
Residual rms (μ s)	46	42	36	86	116
EFAC	1.20	1.33	1.35	1.08	1.55
Reference Epoch (MJD)	54000	54000	54000	54000	54000
Timing parameters					
α (J2000)	17 ^h 48 ^m 52 ^s .95290(8)	17 ^h 48 ^m 51 ^s .64665(7)	17 ^h 48 ^m 52 ^s .3339(3)	17 ^h 50 ^m 13 ^s .8016(5)	17 ^h 50 ^m 12 ^s .1770(4)
δ (J2000)	–20°21′38″.86(19)	–20°21′07″.414(18)	–20°21′39″.33(9)	–37°03′10″.95(2)	–37°03′22″.93(2)
ν (Hz)	59.665418222544(17)	74.097014488305(13)	263.5998326931(2)	8.96050624775(3)	164.62146212170(16)
$\dot{\nu}$ (10 ^{–15} Hz s ^{–1})	1.1717(6)	–3.2216(9)	0.733(13)	–0.4545(6)	–0.520(11)
DM (cm ^{–3} pc)	220.922(11)	224.98(3)	220.43(8)	233.82(3)	234.391(9)
P_b (d)	20.5500072(6)	0.2860686769(4)	9.83396979(8)	17.3342759(7)	3.60511446(5)
x (l-s)	4.466994(6)	0.397203(3)	9.497573(11)	24.39312(8)	2.865858(13)
T_0 (MJD)	54005.480292(7)	54000.1053987(3)	54005.80617(6)	54003.127812(11)	54002.7705(11)
e	0.5701606(15)	[0.0]	0.053108(3)	0.712431(2)	0.004046(9)
ω (°)	314.31935(13)	0	191.500(2)	131.3547(2)	323.07(11)
$\dot{\omega}$ (° yr ^{–1})	0.00391(18)	0.00548(30)	...
Derived parameters					
f (M_\odot)	0.0002266235(9)	0.000822203(16)	0.00951180(3)	0.0518649(5)	0.00194450(3)
M (M_\odot)	2.92(20)	1.97(15)	...
$M_{p,\max}$ (M_\odot)	3.25	1.65	...
$M_{c,\min}$ (M_\odot) ^a	0.11	0.12	0.30	0.53	0.17

^a Calculated assuming a pulsar mass of 1.4 M_\odot . Where a $\dot{\omega}$ was measured, these limits include 99% of the total probability.

Damour & Deruelle 1986). The reference epoch for all solutions is MJD = 54000 (2006 September 9). The timing solution of NGC 6440B is the only one that includes the “mode 14” data taken in October 2007; all the others include only mode 2 data, which ends in 2007 March 28.

The 3-level sampling of the Spigot introduces systematics on the profiles that are not well understood. Following standard pulsar timing practice in such cases, we compensate for this by increasing the uncertainties on the TOAs by the small factor indicated in Tables 3 and 4 as “EFAC”, such that the reduced $\chi^2 = 1$. In all cases except that of NGC 6440C, these factors are small, indicating that the timing models in Tables 3 and 4 do a good job of predicting the rotational phases of the pulsars, i.e., there are no unmodeled trends in the TOA

residuals (for two examples, see Fig. 3). For this reason, we believe that the 1- σ uncertainty estimates returned by TEMPO are essentially accurate, so they are reported directly in Tables 3 and 4. In §4.3, we test the validity of this hypothesis for the measurement of the $\dot{\omega}$ of NGC 6440B.

The large EFAC of NGC 6440C indicates the presence of unmodeled effects in its TOA residuals. The cause of these is unknown at present, and will be investigated elsewhere.

3.1. Positions

In Table 5, we calculate the angular offsets of the pulsar positions listed in Tables 3 and 4 relative to the centers of their respective GCs listed in Table 2. These are dis-

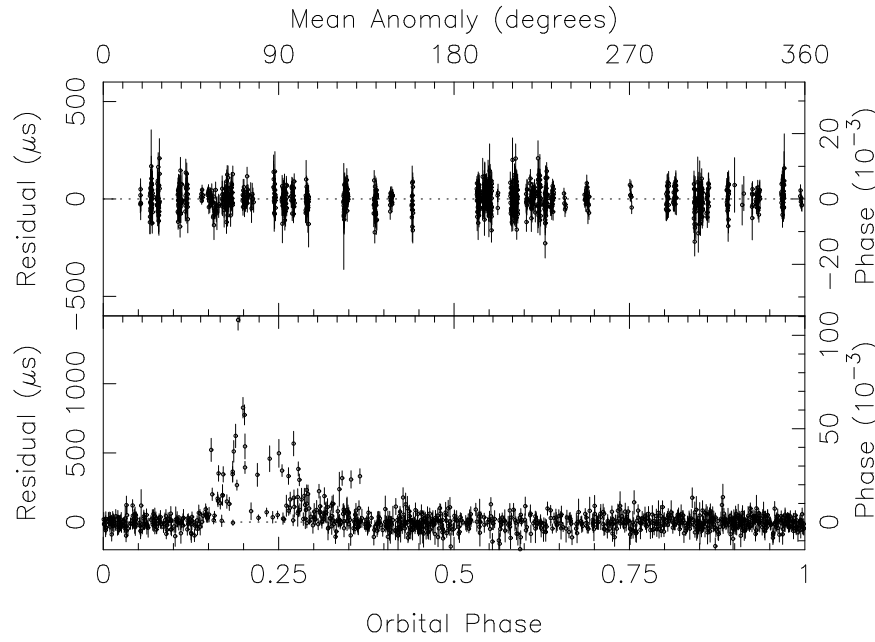


FIG. 3.— Time of arrival residuals as a function of orbital phase for NGC 6440B (*top*) and NGC 6440D (*bottom*).

TABLE 5
PULSAR OFFSETS FROM THE CENTERS OF
NGC 6440 AND NGC 6441

Pulsar	$\theta_\alpha^{a,b}$ ($^\circ$)	θ_δ^a ($^\circ$)	θ_\perp ($^\circ$)	θ_c ($^\circ$)	r_\perp (pc)
NGC 6440					
A ...	-0.0017	-0.0447	0.04	0.34	0.11
B ...	0.0601	-0.0307	0.07	0.52	0.16
C ...	-0.3571	-0.2801	0.45	3.49	1.08
D ...	-0.2472	0.4930	0.55	4.24	1.32
E	0.0240	0.1269	0.13	0.99	0.31
F	-0.0858	-0.0389	0.09	0.72	0.22
NGC 6441					
A ...	0.1797	-0.0993	0.21	1.87	0.81
B ...	-0.1432	-0.2989	0.33	3.01	1.30
C ...	0.1111	-0.0096	0.11	1.01	0.44
D ...	0.0395	-0.0229	0.05	0.41	0.18

^a The uncertainty of these parameters is much smaller than the uncertainty of the position of the center of the GC (they were computed assuming that the center is *exactly* where indicated in Table 2). This precision is, however, necessary to calculate the angular distances between the pulsars.

^b Note that $\theta_\alpha = d\alpha \cos \delta$, where $d\alpha$ is the difference of the Right Ascension of the pulsar and the center of the GC.

played graphically in the top panels of Figures 4 and 5. The projected distances of the pulsars from the center of the GC (r_\perp) were calculated using the most recent GC distance estimates listed in Table 2. There is nothing unusual about the spatial distribution of the pulsars in these GCs. As in 47 Tucanae and most other GCs, all pulsars are located within the half-mass radius of the GC (Camilo & Rasio 2005); in the present cases at less than 0'6 (or 4.5 core radii) from the center. This is not an observational bias: the S-band telescope beam still has >50% sensitivity 3' from the center of the GC. Furthermore, the 820-MHz observations do not reveal any extra pulsars within $\sim 8'$ from the center of the GC. The con-

gregation of pulsars at the center is a real phenomenon, due to mass segregation in the GC.

3.2. Period derivatives

In the third column of Table 6, we list the observed period derivatives (\dot{P}_{obs}). Four effects can contribute to \dot{P}_{obs} (Phinney 1993):

$$\left(\frac{\dot{P}}{P}\right)_{\text{obs}} = \left(\frac{\dot{P}}{P}\right)_{\text{int}} + \frac{1}{c}(a_G + a_{GC} + a_{PM}), \quad (3)$$

where \dot{P}_{int} is the pulsar's intrinsic period derivative, a_{GC} is the line-of-sight component of the acceleration of the pulsar caused by the gravitational field of the GC, a_G is the difference of the accelerations of the GC and of the Solar System in the gravitational field of the Galaxy, projected along the line of sight, $a_{PM} = \mu^2 D$ (Shklovskii 1970) is the centrifugal acceleration due to the transverse motion of the pulsar μ , and D is the GC's distance from the Earth, listed in Table 2. The pulsar proper motions μ are not yet directly measurable, and there are no optical measurements of the proper motions of the two GCs; so, like \dot{P}_{int} , a_{PM} is not known but is always positive.

In the fourth column of Table 6, we list the observational upper limits for the pulsar acceleration, $a_{p,\text{max}}$, obtained by re-arranging all the known terms of Eq. 3 to the right side of the equation:

$$a_{p,\text{max}} \equiv a_{GC} + c \left(\frac{\dot{P}}{P}\right)_{\text{int}} + \mu^2 D = c \left(\frac{\dot{P}}{P}\right)_{\text{obs}} - a_G. \quad (4)$$

We calculated a_G using a mass model of the Galaxy (Kuijken & Gilmore 1989), the estimated distance to the GCs, and their Galactic coordinates given in Table 2.

TABLE 6
LIMITS FOR DERIVED PARAMETERS OF THE NGC 6440 AND NGC 6441 PULSARS

Pulsar	P (ms)	\dot{P}_{obs} (10^{-18})	$a_{p,\text{max}}$ (10^{-9})	$a_{GC,\text{max}}$ (m s^{-2})	$\dot{P}_{\text{int,max}}$ (10^{-18})	$\dot{P}_{\text{int,min}}$ (10^{-18})	B_{max} (10^9 G)	B_{min} (10^9 G)	$\tau_{c,\text{max}}$ (Gyr)	$\tau_{c,\text{min}}$ (Gyr)
NGC 6440										
A ...	288.6027917197(16)	399.33(10)	414.8	26.30	424.7	374.0	353.2	331.4	0.012	0.011
B ...	16.760127219257(5)	-0.32913(16)	-5.86	24.72	1.05	(0.0)	4.24	(0.0)	($+\infty$)	0.25
C ...	6.226932720487(2)	-0.05984(16)	-2.85	6.15	0.07	(0.0)	0.66	(0.0)	($+\infty$)	1.45
D ...	13.495820403909(2)	0.58678(16)	13.06	4.77	0.80	0.37	3.32	2.26	0.57	0.27
E	16.264003411125(5)	0.3124(4)	5.79	19.62	1.38	(0.0)	4.78	(0.0)	($+\infty$)	0.19
F	3.793629114949(3)	-0.01055(18)	-0.81	22.53	0.27	(0.0)	1.03	(0.0)	($+\infty$)	0.22
NGC 6441										
A ...	111.6008373133(4)	5.661(8)	15.67	19.88	13.2	(0.0)	38.8	(0.0)	($+\infty$)	0.13
B ...	6.074542086503(6)	0.0192(4)	1.41	11.88	0.27	(0.0)	1.29	(0.0)	($+\infty$)	0.36
C ...	26.56867837497(4)	-0.996(3)	-10.77	31.30	1.82	(0.0)	7.01	(0.0)	($+\infty$)	0.23
D ...	5.139936774902(4)	0.4928(2)	29.20	41.46	1.21	(0.0)	2.52	(0.0)	($+\infty$)	0.067

Since we have no estimates of the proper motion of the GCs, we assume from now on that $\mu^2 D = 0$. In all GCs where this term is measured, it is small relative to the intrinsic period derivatives and even smaller compared to the accelerations induced by the GC.

In the fifth column we list the theoretical maximum value of a_{GC} for each pulsar’s line-of-sight, $a_{GC,\text{max}}$. This is calculated using an analytical mass model for the centers of GCs described in the Appendix of Freire *et al.* (2005), using the core radius and central velocity dispersion listed in Table 2. Both $a_{p,\text{max}}$ for the individual pulsars and $a_{GC,\text{max}}$ for all lines of sight close to the center of the GC are displayed in the bottom halves of Figures 4 and 5.

Using Eq. 4, we can calculate upper (and, in the cases of NGC 6440A and D, lower) limits for \dot{P}_{int} assuming the extreme possible accelerations $\pm a_{GC,\text{max}}$. These limits are displayed in the sixth and seventh columns of Table 6. From these \dot{P}_{int} limits, we can calculate upper and lower limits for the magnetic field at the surface (estimated using $B_0 = 3.2 \times 10^{19} (P \dot{P}_{\text{int}})^{1/2}$ G) and lower and upper limits for the characteristic age of these pulsars (estimated using $\tau_c = P/2\dot{P}_{\text{int}}$), these are displayed in the final columns of Table 6. No pulsar in either GC has $a_{p,\text{max}} < -a_{GC,\text{max}}$, this means that the present GC mass models can predict line-of-sight accelerations large enough to explain the observed negative period derivatives (and plausibly maintain that the pulsars are not spinning up).

3.2.1. NGC 6440A

As previously found by Lyne, Manchester & D’Amico (1996), PSR B1745–20A has a characteristic age $\sim 10^3$ times smaller than the age of the GC and $B_0 \sim 3 \times 10^{11}$ G, a value that is more typical of what one finds in the general Galactic population. For these two reasons, there have been some doubts about the association of this pulsar with NGC 6440. The discovery of five new MSPs in NGC 6440 at DMs similar to that of PSR B1745–20A confirms its association with NGC 6440. Furthermore, PSR B1745–20A is closer to the center of the GC ($\theta_{\perp} = 0'.04$) than any of the new MSPs.

This association of a “young” pulsar with a GC is not unique to NGC 6440. The first known examples were PSR B1718–19, in NGC 6342 (Lyne *et al.* 1993) and PSR B1820–30B in NGC 6624 (Biggs *et al.* 1994).

The possible origins of these objects, and in particular NGC 6440A, are discussed in detail in Lyne, Manchester & D’Amico (1996). Either neutron star formation continues to happen in GCs — through electron capture supernovae (ECS), which can form when an accreting WD star reaches the Chandrasekhar limit or when a WD binary coalesces — or some form of mild recycling happened, in which the pulsar was not spun up to very short spin periods and not much of its magnetic field was buried. The ECS scenario is particularly appealing as this type of supernova also produces small kicks, which nicely solves the problem of neutron star retention in GCs (Ivanova *et al.* 2007).

3.2.2. NGC 6440D

Unlike in the case of NGC 6440A, the upper limit for τ_c and the lower limit for B does not imply that this pulsar is younger or has a stronger magnetic field than the other MSPs. It is possible that the other “slow MSPs” (with $13 < P < 27$ ms) have similar ages and magnetic fields as those of NGC 6440D; their intrinsic \dot{P} s might simply be masked by the GC accelerations. The apparently special limits for NGC 6440D might have more to do with its large distance from the center of the GC: the range of possible GC accelerations $a_{GC,\text{max}}$ is the smallest for all pulsar positions in NGC 6440 and NGC 6441; this leads to tighter limits on \dot{P}_{int} . If NGC 6440D is a typical slow MSP, then the magnetic fields of these objects are one order of magnitude larger than those observed in 47 Tucanae (Freire *et al.* 2001); this would cause the observed difference in spin periods between GCs discussed in §2.2.

4. BINARY SYSTEMS

Before this survey, only one binary pulsar was known in these two GCs, NGC 6441A (Possenti *et al.* 2006). We have discovered four new binary systems, three in NGC 6440 (B, D and F) and one in NGC 6441 (B). These binaries make up half of the total observed pulsar population in these GCs. This ratio is similar to that of Terzan 5, but significantly lower than what we find in 47 Tucanae and M62, in the latter GC all the 6 known pulsars are in binary systems.

4.1. NGC 6440F and NGC 6441B

These two binaries, with orbital periods of 9.8 and 3.6 d and minimum companion masses of 0.30 and $0.17 M_{\odot}$

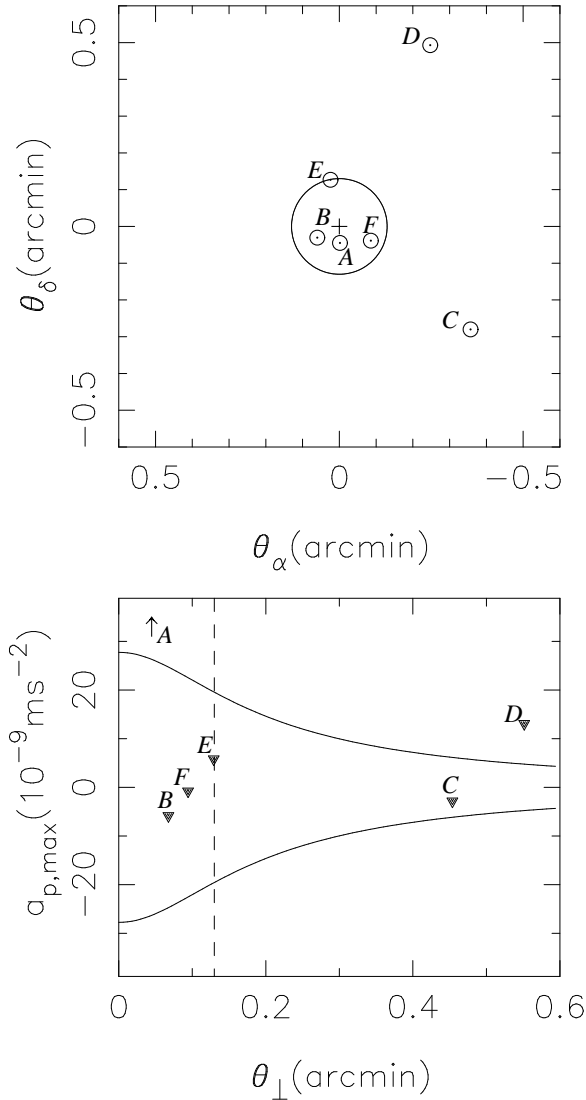


FIG. 4.— *Top*: Positions of the six known pulsars in NGC 6440, plotted as west-east (θ_α) and south-north (θ_δ) offsets from the center of the GC (see also Table 5). The angular core radius ($\theta_c = 0'.13$) is represented by a circle. *Bottom*: Upper limits for the accelerations of the MSPs (triangles). These are compared with the maximum acceleration that can be caused by the GC, as a function of θ_\perp (solid curves). The angular core radius is indicated by the vertical dashed line. Pulsar NGC 6440A, and to a much lesser extent NGC 6440D are significantly above the maximum GC acceleration, indicating that its large positive \dot{P} is caused by its intrinsic slowdown.

respectively (assuming pulsar masses of $1.4 M_\odot$), might be the only “normal” MSP-WD binaries among the new pulsars. Their spin periods (3.79 and 6.07 ms) are at the lower end of the spin period distribution found in NGC 6440 and NGC 6441, but they are typical of what is found among similar MSP-WD binaries in other GCs and in the Galactic disk. Their eccentricities (0.0531 and 0.00404) are small compared to the highly eccentric NGC 6440B and NGC 6441A, but they are nevertheless much larger than what is found in binary systems with similar orbital periods in the Galactic disk. This is a common occurrence in GCs, and is probably due to perturbations caused by close flybys of other stars in these GCs (Heggie & Rasio 1996).

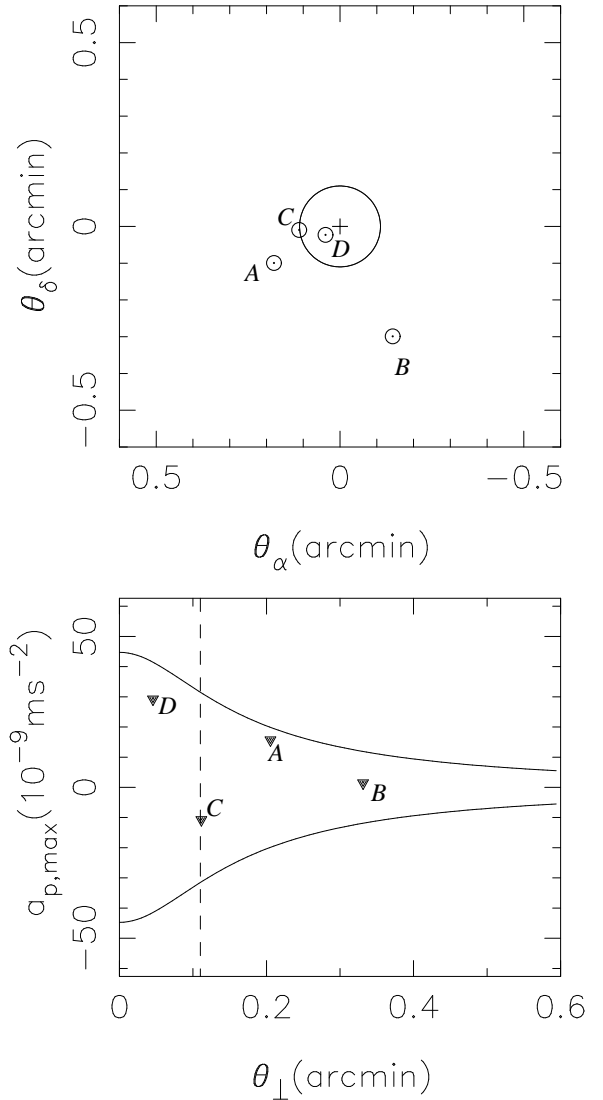


FIG. 5.— *Top*: Same as for the top of Fig. 4 for the four MSPs in NGC 6441. The angular core radius ($\theta_c = 0'.11$) is represented by a circle. *Bottom*: Upper limits on the accelerations of the MSPs in NGC 6441 (triangles) and theoretical maximum acceleration as a function of θ_\perp (solid curves).

4.2. NGC 6440D - Eclipsing binary

The binary system NGC 6440D has an orbit with non-measurable eccentricity and a period of 6.9 hr. It is an eclipsing system with eclipses that usually last for about 10% of the orbital cycle. Its minimum companion mass is $0.12 M_\odot$, calculated assuming a pulsar mass of $1.4 M_\odot$. Freire (2005) called attention to the fact that eclipsing binary pulsars have a bi-modal distribution of mass functions: those with $f > 10^{-4} M_\odot$ were designated “Eclipsing Low-Mass Binary Pulsars” (ELMBPs), while those with $f < 3 \times 10^{-5} M_\odot$ were designated as “Very Low-Mass Binary Pulsars” (VLMBPs). The VLMBPs are more commonly known as “Black Widow” pulsars. NGC 6440D is clearly a ELMBP. Unlike “Black Widows”, these objects only occur in GCs, suggesting that they form through exchange interactions when a radio pulsar acquires a MS companion.

Sometimes NGC 6440D is detectable during superior

conjunction. This indicates that the orbital inclination is certainly less than 90° , otherwise the companion itself would cause an eclipse. It also implies that the concentration of the material producing the eclipse is highly variable with time. Nevertheless, the cloud of material seems to generally lead the companion in orbital phase (see Fig. 3), i.e., ingress occurs at a much larger distance from superior conjunction than egress. Before, after, and sometimes through the eclipse we detect ~ 0.5 ms delays in the times of arrival (see Fig. 3). These are probably due to an increase in the electron column density near the companion of up to $\sim 0.5 \text{ cm}^{-3} \text{ pc}$ (or about $1.5 \times 10^{18} \text{ cm}^{-2}$). This is of the same order of magnitude as what has been found in similar binary systems, e.g. M30A (Ransom *et al.* 2004).

If the system is nearly edge on, with pulsar and companion masses of 1.4 and $0.124 M_\odot$, the separation between the stellar components is $1.47 \times 10^{11} \text{ cm}$ ($2.1 R_\odot$). On some occasions the eclipse extends up to $\sim 30^\circ$ from superior conjunction (normally before the companion), which implies the detection of material at $\sim 1.0 R_\odot$ from the center of the companion. The size of the Roche lobe of the companion is $0.42 R_\odot$, therefore, it is clear that we are detecting the presence of material that is not bound to the companion at ingress. We almost never detect unbound material at egress.

This is different from what one observes in ELMBPs such as 47 Tuc W (Camilo *et al.* 2000), Terzan 5 P and ad (Ransom *et al.* 2005; Hessels *et al.* 2006), PSR J1740–5340 in NGC 6397 (D’Amico *et al.* 2001) or M28 H (Bégin 2006; Bégin *et al.* in preparation), which display long duration irregular eclipses likely related to excessive unbound ionized material from the companion over much of the orbit. Three of these ELMBP companions have been identified at optical wavelengths (47 Tuc W, Edmonds *et al.* 2002, ; PSR B1718–19 in NGC 6349, Kerkwijk *et al.* 2000; and PSR J1740–5340 in NGC 6397, Ferraro *et al.* 2001), and in all cases the observed companion is a low-mass, non-degenerate star. None of the ELMBPs with shorter eclipses such as M30 A, Terzan 5 A (Lyne *et al.* 1990) and M62 B (Possenti *et al.* 2003) have been optically detected. The situation is similar at X-rays: only the systems with large eclipses have been detected (e.g., 47 Tuc W, see Bogdanov, Grindlay & van den Berg 2006). In these systems the hard X-ray emission is generated by the collision of MSP and stellar winds. None of the ELMBPs with shorter eclipses have been definitively detected at X-ray wavelengths. If NGC 6440D is similar to these ELMBPs, it seems less likely that it will be detected at either optical or X-ray wavelengths.

When an exchange encounter forms a ELMBP, the ejection of the previous companion to the pulsar imparts a kick to the binary, making it fly away from the central regions of the GC in an eccentric orbit. It is probably for that reason that two ELMBPs (PSR B1718–19 and PSR J1740–5340) are found at large distances from the centers of their parent GCs (Freire 2005). NGC 6440D follows this trend: of all the pulsars in NGC 6440 and NGC 6441, it is farthest from the center of its GC as projected on the plane of the sky.

4.3. NGC 6440B: eccentric binary with a super-massive neutron star?

NGC 6440B and NGC 6441A (§4.4) are part of a diverse class of binary pulsars in GCs with eccentric orbits that includes mostly recent discoveries like M30B (Ransom *et al.* 2004), NGC 1851A (Freire *et al.* 2004; Freire *et al.* 2007), six systems in Terzan 5 (I, J, Q, U, X and Z; Ransom *et al.* 2005; Stairs *et al.*, in preparation) and M28 C and D (Bégin 2006; Bégin *et al.* in preparation). With the exception of M15C (Jacoby *et al.* 2006), which is very similar to some DNSs seen in the Galaxy, they have no Galactic analogues. All of these systems were likely formed through stellar exchange encounters.

The orbital eccentricity of NGC 6440B has allowed a highly significant measurement of the rate of advance of periastron: $\dot{\omega} = 0.00391(18)^\circ \text{ yr}^{-1}$. As mentioned above, this is a $1\text{-}\sigma$ uncertainty derived by TEMPO. To check if this uncertainty value is realistic, we estimated $\dot{\omega}$ and its associated uncertainty using two other methods. First, all the timing parameters of NGC 6440B were estimated using a Monte-Carlo Bootstrap algorithm (Efron & Tibshirani 1993; Press *et al.* 1992), with a total of 1024 fake TOA datasets that are consistent with the real dataset. From this we obtain $\dot{\omega} = 0.00391(16)^\circ \text{ yr}^{-1}$. In the second estimate, we kept $\dot{\omega}$ fixed and fitted all the remaining timing parameters, recording the resulting χ^2 . Doing this for a range of values of $\dot{\omega}$, we can estimate the $1\text{-}\sigma$ uncertainty as the half-width of the region where $[\chi^2(\dot{\omega}) - \chi^2(\dot{\omega}_{\min}) < 1]$, being $\dot{\omega}_{\min}$ the value that minimizes χ^2 (Splaver *et al.* 2002). The result of this estimate is $\dot{\omega} = 0.00391(18)^\circ \text{ yr}^{-1}$. Both these estimates indicate that, at least for the $\dot{\omega}$ of NGC 6440B, the $1\text{-}\sigma$ TEMPO uncertainty is reliable.

The orbital coverage of the timing data is excellent (see Fig. 3): the orbit was well sampled at the end of 2005, at the start of 2007 and again during October 2007. For this reason, $\dot{\omega}$ is not strongly correlated to any timing parameter: its largest correlation is with P_b (96%), which is normal for this particular parameter.

4.3.1. Mass estimate from periastron advance

Assuming that $\dot{\omega}$ is fully relativistic (an important assumption, as we will see) implies a total system mass of $2.92 \pm 0.20 M_\odot$. This binary system is located, at least in projection, close to the center of the GC, where the massive objects should predominantly occur. In Figure 6, we present the mass constraints on the components graphically. We assume that the probability density function (pdf) for $\dot{\omega}$, $p(\dot{\omega})$, is a Gaussian, with half-width similar to the 1σ uncertainty given by TEMPO. We also assume a constant probability density for $\cos i$, where i is the orbital inclination (90° for an edge-on orbit). From these constraints, we calculate a two-dimensional pdf for the mass of the pulsar and the mass of the companion. This is then projected in both dimensions, resulting in final pdfs for the mass of the pulsar and the mass of the companion.

The total mass of this system suggests that it is a double neutron star (DNS) binary. However, the probability that the pulsar lies within the range of neutron star masses that have been precisely measured to date — from $\sim 1.20 M_\odot$ for the companion of PSR J1756–2251 (Faulkner *et al.* 2005) to $1.44 M_\odot$ for PSR B1913+16 (Weisberg & Taylor 2003), indicated in Figures 6 and 7 by grey bars — is only 0.10%. This eventuality would

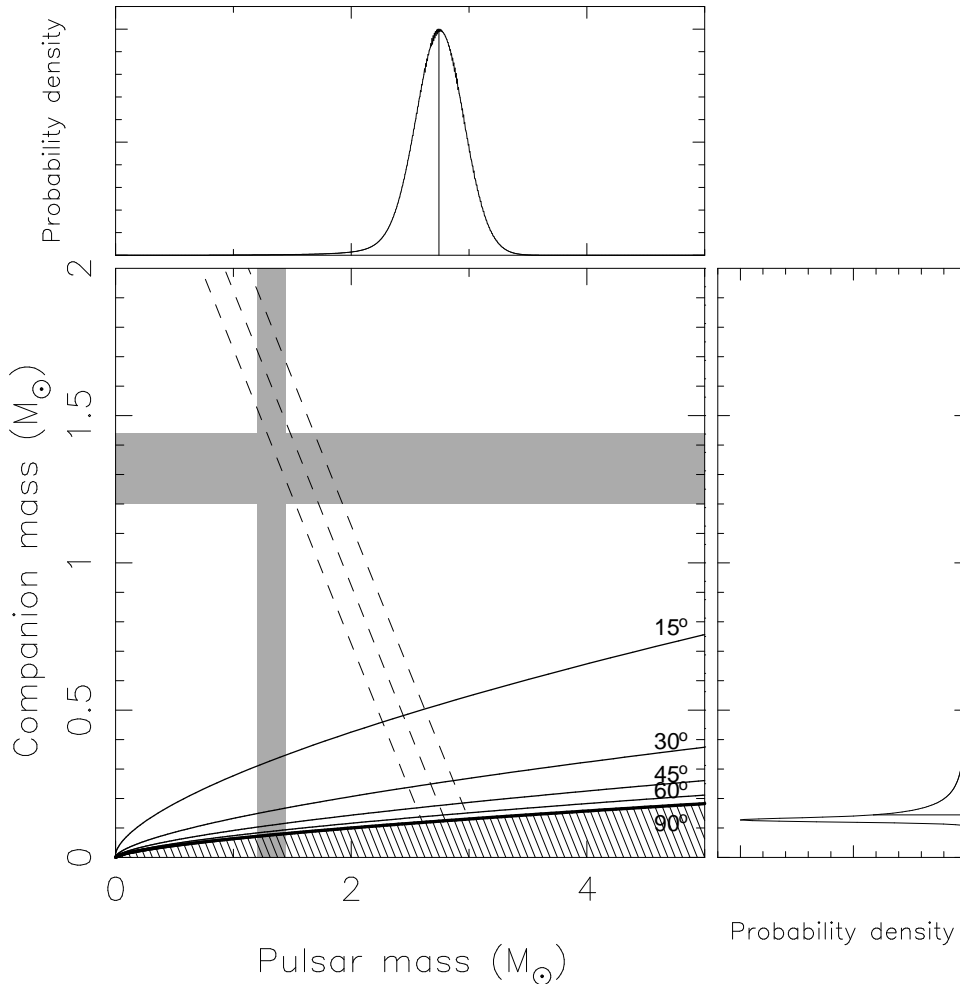


FIG. 6.— Graphical display of the constraints on the masses of NGC 6440B and its companion. In the main display, the hatched region is excluded by knowledge of the mass function and by $\sin i \leq 1$. The slanting straight lines correspond to a total system mass that causes a general-relativistic $\dot{\omega}$ equal or within 1σ (dashed lines) of the measured value. The five solid curves indicate constant orbital inclinations. The gray bars indicates the range of precisely measured neutron star masses. We also display the probability density function for the mass of the pulsar (top) and the mass of the companion (right), and mark the respective medians with vertical (horizontal) lines.

require very low orbital inclinations, between $\sim 4^\circ$ and $\sim 5^\circ$. In this inclination range, it is also possible that the pulsar has a blue straggler companion, a possibility that can be investigated using optical/IR imaging.

Before this study, the most massive neutron star known was PSR B1516+02B in the GC M5 ($1.96^{+0.09}_{-0.12} M_{\odot}$; Freire et al. 2007). If NGC 6440B had a similar mass, then the companion could be a $\sim 0.9 M_{\odot}$ white dwarf, or a blue straggler of similar mass. However, we note that there is only a 0.97% probability that the mass of the pulsar is below $2.0 M_{\odot}$.

The median pulsar mass is $2.74 M_{\odot}$, with the lower and upper 1σ limits at 2.52 and $2.95 M_{\odot}$, and the 2σ limits at 2.23 and $3.15 M_{\odot}$. The pulsar has a 99% probability of being less massive than $3.24 M_{\odot}$. For the companion, the median of the distribution is at $0.142 M_{\odot}$, with the lower and upper 1σ limits at 0.124 and $0.228 M_{\odot}$, and the 2σ limits at 0.113 and $0.571 M_{\odot}$, implying that it could be a low-mass WD or an un-evolved MS star. If this high pulsar mass is confirmed, it would be by far the largest neutron star mass ever measured. That would have profound consequences for the study of

the equation of state of dense matter, since almost no models predict neutron stars more massive than $2.5 M_{\odot}$ (Lattimer & Prakash 2007).

If NGC 6440B really has a mass of $\sim 2.7 M_{\odot}$, it would imply that the end products of the coalescence of DNS systems might themselves be stable as super-massive neutron stars. The total masses of the known DNS systems range from $2.57 M_{\odot}$ (Faulkner et al. 2005) to $2.83 M_{\odot}$ (Weisberg & Taylor 2003). Such coalescence products might be observable after coalescence, either through gravitational wave emission (Andersson 2003), cooling through neutrino emission (direct URCA process, Page & Applegate 1992) or even high-energy blackbody emission.

It is possible that NGC 6440B itself formed this way. M15C, the only DNS known in the GC system (Jacoby et al. 2006), is expected to coalesce in about 3×10^8 years ($\sim 3\%$ of the age of M15). If the products of DNS coalescence are as likely to be detected as radio pulsars as their progenitors, then we should detect ~ 30 of them in the whole GC system. It is possible that some isolated MSPs in GCs and the Galactic disk formed this way. The massive isolated MSPs in GCs can

later acquire a companion through exchange encounters, forming a system like NGC 6440B where we can measure their large masses.

4.3.2. *Is the periastron advance relativistic?*

The previous discussion rests on the assumption that the observed $\dot{\omega}$ is fully relativistic. If there was an extra contribution to $\dot{\omega}$ from tidal or rotational deformation of the companion, then no reliable estimates can be made of the total mass of the system.

Lai, Bildsten & Kaspi (1995), in their analysis of the binary pulsar PSR J0045–7319, concluded that the only likely contribution to $\dot{\omega}$ in that system is from rotational deformation of the companion. NGC 6440B has a shorter orbital period than PSR J0045–7319 (20.5 versus 51 days), but it also has a much smaller companion mass ($\sim 0.12 M_{\odot}$ at $i = 90^{\circ}$ to $\sim 1.5 M_{\odot}$ at $i \sim 4 - 5^{\circ}$) versus $\sim 9 M_{\odot}$ for the companion of PSR J0045–7319 (Bell et al. 1995). Main-sequence stars of such masses have radii of $R \sim 0.18 - 1.5$ and $\sim 4.5 R_{\odot}$ respectively (Lang 1991). This implies that even if the companion of NGC 6440B were extended, the contribution to $\dot{\omega}$ from its tidal deformation (the latter proportional to $(R/a)^3$, where a is the separation between components) would always be smaller for NGC 6440B than it is for PSR J0045–7319.

The only possible exception to this is if the companion of NGC 6440B were a $\sim 0.9 M_{\odot}$ star undergoing a pre-giant or giant phase. Given the mass function of the system, that would require a very low orbital inclination. A giant star of that mass would have a radius of up to 1 a.u. (Lang 1991), and would not fit in the space between the pulsar and companion at any orbital phase. If it were in a “pre-giant” phase, its atmosphere would be very extended and have significant mass loss, leading to variations in the DM with orbital phase. The resulting tides should not only have circularized the orbit, but they should also have directly observable effects on the timing: unmodeled effects in the rotation of the pulsar and random variations of the orbit’s period and apparent size (Nice, Arzoumanian & Thorsett 2000). For PSR J0045–7319, there is strong orbital decay due to tidal effects (Kumar & Quataert 1998).

For NGC 6440B, we obtain $\dot{P}_b = (-0.0 \pm 1.4) \times 10^{-9}$ and $\dot{x} = (-0.21 \pm 0.14) \times 10^{-12}$. The pulsar times very well, with an EFAC similar to those of the isolated MSPs in the GC (see Table 4), no unmodeled systematic trends are visible in the TOA residuals (Fig. 3). Fitting for the halves of the orbit “in front” and “behind” the companion, we see no DM variations larger than our detection limit of $0.07 \text{ cm}^{-3} \text{ pc}$. The possibility of an unusually extended companion to NGC 6440B and of a significant tidal contribution to $\dot{\omega}$ can be safely excluded.

The contribution from rotational deformation, henceforth designated as $\dot{\omega}_{\text{rot}}$, could be significant if the companion (degenerate or not) were spinning rapidly. The rotational deformation will also induce a change in the projected semi-major axis of the orbit \dot{x} . Splaver et al. (2002), based on the results of Lai, Bildsten & Kaspi (1995) and Wex (1998), relate $\dot{\omega}_{\text{rot}}$ to \dot{x} :

$$\dot{\omega}_{\text{rot}} = \frac{\dot{x}}{x} \left(\tan i \frac{1 - \frac{3}{2} \sin^2 \theta}{\sin \theta \cos \theta \sin \Phi_0} + \cot \Phi_0 \right), \quad (5)$$

where i is the orbital inclination of the binary, θ is the angle between the angular momentum vector of the secondary and the angular momentum vector of the orbit; and Φ_0 is the longitude of the ascending node in a reference frame defined by the total angular momentum vector (see Fig. 9 of Wex 1998).

Thus, our observed upper limit of $|\dot{x}/x| < 8 \times 10^{-14}$ implies $|\dot{\omega}_{\text{rot}}| < 1.5 \times 10^{-4} \text{ yr}^{-1}$ times a geometric factor. In 80% of cases this geometric factor will be smaller than 10. Therefore $\dot{\omega}_{\text{rot}}$ will in most cases be of the same order of magnitude as the present measurement uncertainty for $\dot{\omega}$. Certain special combinations of i , θ , and Φ_0 will make the geometric factor large, but, again, this would only occur if the companion were rotating fast.

To summarize, the contribution to the $\dot{\omega}$ of this system from the tidal deformation of the companion is negligible. Furthermore, observational limits on \dot{x} indicate that $\dot{\omega}_{\text{rot}}$ is also likely to be negligible and the observed $\dot{\omega}$ due to the effects of general relativity.

4.4. *NGC 6441A: eccentric binary with a massive companion*

NGC 6441A was the only pulsar previously known in NGC 6441 (Possenti et al. 2006), although its phase-connected timing solution has never been published. Its orbital period is 17.3 days, and its orbit is highly eccentric ($e = 0.71$), allowing a measurement of the advance of periastron for this system, $\dot{\omega} = 0.00548(30) \text{ yr}^{-1}$. Assuming, again, that this effect is fully due to general relativity, we obtain a total mass of $1.97 \pm 0.15 M_{\odot}$, consistent with the estimate made by Possenti et al. (2006): $2.15 \pm 0.06 M_{\odot}$. Using the methods applied in the case of NGC 6440B, we calculated pdfs for the mass of this pulsar and its companion for our measurement of the total mass of the binary; these are displayed graphically in Figure 7. There is a 99% probability that the companion is more massive than $0.53 M_{\odot}$ and that the pulsar is less massive than $1.65 M_{\odot}$. The medians for the pulsar and companion masses are 1.26 and $0.67 M_{\odot}$ respectively, and there is a 45.6% probability that the pulsar mass is within the 1.20–1.44 M_{\odot} mass range. The nature of the companion is unknown, but no observational hints of tidal effects (\dot{x} , \dot{P}_b , DM variations) are present, suggesting it is a compact object.

5. CONCLUSION AND PROSPECTS

We have discovered eight new pulsars in the GCs NGC 6440 and NGC 6441. Their pseudo-luminosities indicate that there may be as many pulsars in these GCs as in Terzan 5, but less pulsars are observed in the former because of their larger distances. The pulsar population in these GCs seems to have distinctly lower spin frequencies. To some extent, this is due to the presence of apparently young objects like NGC 6440A. At least in the case of NGC 6440A and D, and possibly in the case of the other slow MSPs, the larger spin periods could be related with many of them having higher magnetic fields than the MSPs in other GCs.

Four of the new pulsars are in binary systems. NGC 6440D is an eclipsing binary, with a companion star with a mass of about $0.12 M_{\odot}$ or larger. NGC 6440B is a 16.7-ms pulsar in a 20.5-day orbit with an orbital eccentricity of 0.57. A measurement of the rate of advance of

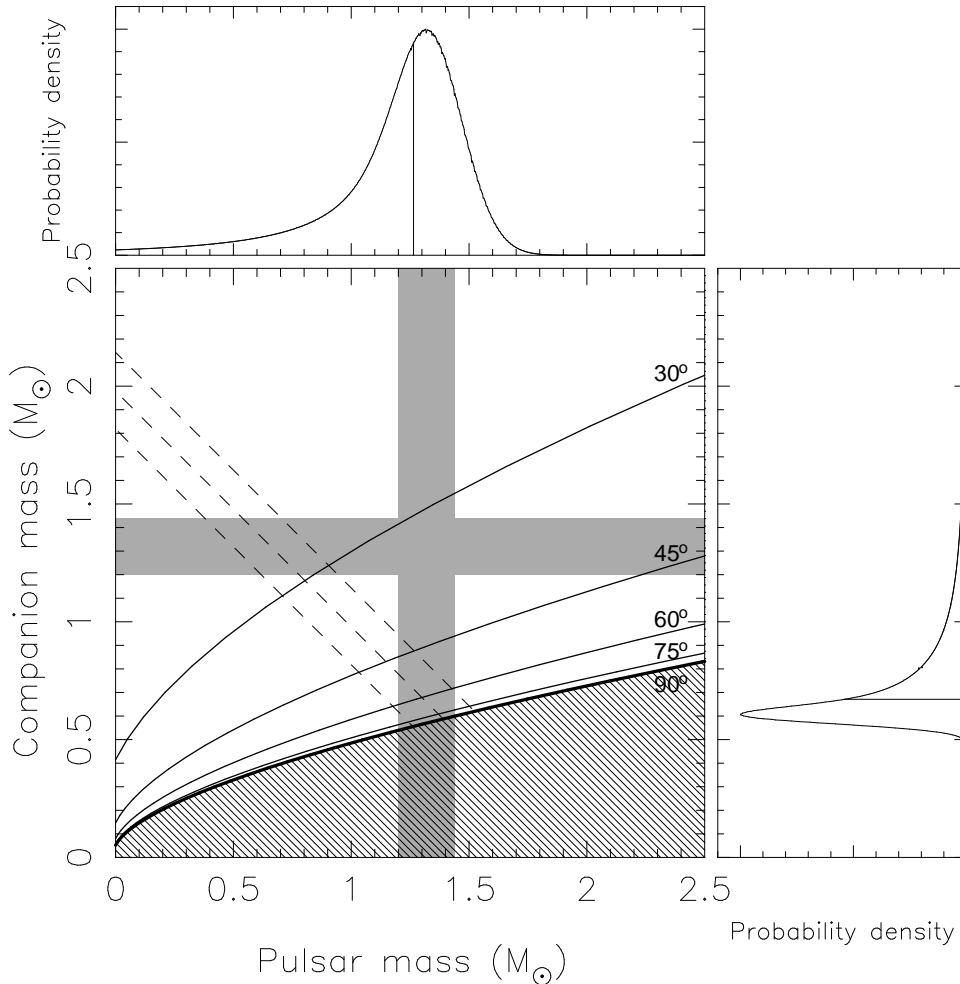


FIG. 7.— Display as in Fig. 6, this time for the NGC 6441A binary system.

periastron for this system suggests that this binary hosts the most massive neutron star to date: $2.74 \pm 0.21 M_{\odot}$, with only a 1% probability that the inclination is low enough that pulsar mass is below $2 M_{\odot}$. This result depends on the (likely) possibility that the observed periastron advance is fully relativistic. Such a large mass would introduce the strongest constraints to date on the equation of state; it also suggests that the products of the coalescence of double neutron stars might be stable neutron stars. The rate of advance of periastron was also measured for NGC 6441A, indicating a significantly less massive pulsar ($M_p < 1.65 M_{\odot}$).

The pulsars in NGC 6440 will be monitored carefully over the next few years. In the case of NGC 6440C, the new data will allow a detailed investigation of the origin of its timing irregularities. In the case of NGC 6440B, the continued monitoring will lead to an improvement in

the precision of $\dot{\omega}$. Simulations indicate that the Einstein delay (γ) may become measurable with about 15 years of data; this would provide unambiguous mass measurements and determine the nature of the companion. Deep optical studies of NGC 6440 might be extremely valuable in determining the nature of the companion of NGC 6440B.

The National Radio Astronomy Observatory is a facility of the National Science Foundation operated under cooperative agreement by Associated Universities, Incorporated. IHS held an NSERC UFA while most of this work was performed and pulsar research at UBC is supported by a Discovery Grant. JWTH holds an NSERC PDF and CSA supplement. LHF's work for this paper was sponsored by the Research Experience for Undergraduates program of the NSF.

REFERENCES

- Andersson, N. 2003, *Classical and Quantum Gravity*, 20, 105
 Bégin, S. 2006. Master's thesis, University of British Columbia
 Bégin, S., Ransom, S. M., Freire, P. C. C., Stairs, I. H., Hessels, J. W. T., Katz, J., Kaspi, V., & Camilo, F. 2008, *ApJ*. in preparation
 Bell, J. F., Bessell, M. S., Stappers, B. W., Bailes, M., & Kaspi, V. M. 1995, *ApJ*, 447, L117
 Biggs, J. D., Bailes, M., Lyne, A. G., Goss, W. M., & Fruchter, A. S. 1994, *MNRAS*, 267, 125
 Bogdanov, S., Grindlay, J. E., & van den Berg, M. 2005, *ApJ*, 630, 1029
 Camilo, F., Lorimer, D. R., Freire, P., Lyne, A. G., & Manchester, R. N. 2000, *ApJ*, 535, 975

- Camilo, F. & Rasio, F. A. 2005, in *Binary Radio Pulsars*, ed. F. A. Rasio & I. H. Stairs, volume 328 of *Astronomical Society of the Pacific Conference Series*, 147
- Chandler, A. M. 2003. PhD thesis, California Institute of Technology
- D'Amico, N., Possenti, A., Manchester, R. N., Sarkissian, J., Lyne, A. G., & Camilo, F. 2001, *ApJ*, 561, L89
- Damour, T. & Deruelle, N. 1985, *Ann. Inst. H. Poincaré (Physique Théorique)*, 43, 107
- Damour, T. & Deruelle, N. 1986, *Ann. Inst. H. Poincaré (Physique Théorique)*, 44, 263
- Dubath, P., Meylan, G., & Mayor, M. 1997, *A&A*, 324, 505
- Edmonds, P. D., Gilliland, R. L., Camilo, F., Heinke, C. O., & Grindlay, J. E. 2002, *ApJ*, 579, 741
- Efron B., Tibshirani R. J., 1993, *An Introduction to the Bootstrap*, Chapman & Hall, New York
- Faulkner, A. J. et al. 2005, *ApJ*, 618, L119
- Ferraro, F. R., Possenti, A., D'Amico, N., & Sabbi, E. 2001, *ApJ*, 561, L93
- Freire, P. C., Camilo, F., Lorimer, D. R., Lyne, A. G., Manchester, R. N., & D'Amico, N. 2001, *MNRAS*, 326, 901
- Freire, P. C., Gupta, Y., Ransom, S. M., & Ishwara-Chandra, C. H. 2004, *ApJ*, 606, L53
- Freire, P. C., Kramer, M., Lyne, A. G., Camilo, F., Manchester, R. N., & D'Amico, N. 2001, *ApJ*, 557, L105
- Freire, P. C. C. 2005, in *ASP Conf. Ser. 328: Binary Radio Pulsars*, ed. F. A. Rasio & I. H. Stairs, 405
- Freire, P. C. C., Hessels, J. W. T., Nice, D. J., Ransom, S. M., Lorimer, D. R., & Stairs, I. H. 2005, *ApJ*, 621, 959
- Freire, P. C. C., Ransom, S. M., & Gupta, Y. 2007, *ApJ*, 662, 1177
- Freire, P. C. C., Wolszczan, A., van den Berg, M. & Hessels, J. W. T. 2007, *ApJ*, submitted, MS#73204
- Harris, W. E. 1996, *AJ*, 112, 1487. Updated version at <http://www.physics.mcmaster.ca/resources/globular.html>
- Heggie, D. C. & Rasio, F. A. 1996, *MNRAS*, 282, 1064
- Hessels, J. W. T., Ransom, S. M., Stairs, I. H., Freire, P. C. C., Kaspi, V. M., & Camilo, F. 2006, *Science*, 311, 1901
- Hessels, J. W. T., Ransom, S. M., Stairs, I. H., Kaspi, V. M., & Freire, P. C. C. 2007, *ApJ*, 670, 363
- Ivanova, N., Heinke, C., Rasio, F. A., Belczynski, K., & Fregeau, J. 2007, *ArXiv e-prints*, 706, arXiv:0706.4096
- Jacoby, B. A., Chandler, A. M., Backer, D. C., Anderson, S. B., & Kulkarni, S. R. 2002. *IAU circular* 7783
- Jacoby, B. A., Cameron, P. B., Jenet, F. A., Anderson, S. B., Murty, R. N., & Kulkarni, S. R. 2006, *ApJ*, 644, L113
- Kaplan, D. L. et al. 2005, *PASP*, 117, 643
- Kuijken, K. & Gilmore, G. 1989, *MNRAS*, 239, 571
- Kumar, P., & Quataert, E. J. 1998, *ApJ*, 493, 412
- Lang, K. R. (1991), "Astrophysical Data: Planets and Stars"; Springer-Verlag, New York.
- Lai, D., Bildsten, L., & Kaspi, V. M. 1995, *ApJ*, 452, 819
- Lyne, A. G., Johnston, S., Manchester, R. N., Staveley-Smith, L., & D'Amico, N. 1990, *Nature*, 347, 650
- Lyne, A. G., Biggs, J. D., Harrison, P. A., & Bailes, M. 1993, 361, 47
- Lyne, A. G., Manchester, R. N., & D'Amico, N. 1996, *ApJ*, 460, L41
- Lattimer, J. M., & Prakash, M. 2007, *Phys. Rep.*, 442, 109
- Nice, D. J., Arzoumanian, Z., & Thorsett, S. E. 2000, in *Pulsar Astronomy - 2000 and Beyond*, IAU Colloquium 177, ed. M. Kramer, N. Wex, & R. Wielebinski, (San Francisco: Astronomical Society of the Pacific), 67
- Nice, D. J. & Thorsett, S. E. 1992, *ApJ*, 397, 249
- Ortolani, S., Barbuy, B., Bica, E., Zoccali, M., & Renzini, A. 2007, *ArXiv e-prints*, arXiv:0705.4030
- Page, D., & Applegate, J. H. 1992, *ApJ*, 394, L17
- Phinney, E. S. 1993, in *Structure and Dynamics of Globular Clusters*, ed. S. G. Djorgovski & G. Meylan, *Astronomical Society of the Pacific Conference Series*, 141
- Pooley, D. et al. 2003, *ApJ*, 591, L131
- Possenti, A., D'Amico, N., Manchester, R. N., Camilo, F., Lyne, A. G., Sarkissian, J., & Corongiu, A. 2003, *ApJ*, 599, 475
- Possenti, A. et al. 2006, *Chinese Journal of Astronomy and Astrophysics Supplement*, 6, 176
- Press, W. H., Teukolsky, S. A., Vetterling, W. T., & Flannery, B. P. 1992, *Numerical Recipes: The Art of Scientific Computing*, 2nd edition, (Cambridge: Cambridge University Press)
- Ransom, S. M., Eikenberry, S. S., & Middleditch, J. 2002, *AJ*, 124, 1788
- Ransom, S. M., Hessels, J. W. T., Stairs, I. H., Freire, P. C. C., Camilo, F., Kaspi, V. M., & Kaplan, D. L. 2005, *Science*, 307, 892
- Ransom, S. M., Stairs, I. H., Backer, D. C., Greenhill, L. J., Bassa, C. G., Hessels, J. W. T., & Kaspi, V. M. 2004, *ApJ*, 604, 328
- Shklovskii, I. S. 1970, *Soviet Ast.*, 13, 562
- Splaver, E. M., Nice, D. J., Arzoumanian, Z., Camilo, F., Lyne, A. G., & Stairs, I. H. 2002, *ApJ*, 581, 509
- Standish, E. M. 1998, *JPL Planetary and Lunar Ephemerides, DE405/LE405*, Memo IOM 312.F-98-048, (Pasadena: JPL). <http://ssd.jpl.nasa.gov/iau-comm4/de405iom/de405iom.pdf>
- Taylor, J. H. 1992, *Philosophical Transactions of the Royal Society of London*, A, 341, 117
- Valenti, E., Ferraro, F. R., & Origlia, L. 2007, *AJ*, 133, 1287
- van Kerkwijk, M. H., Kaspi, V. M., Klemola, A. R., Kulkarni, S. R., Lyne, A. G., & Van Buren, D. 2000, *ApJ*, 529, 428
- Webbink, R. F. 1985, in *Dynamics of Star Clusters*, IAU Symposium No. 113, ed. J. Goodman & P. Hut, (Dordrecht: Reidel), 541
- Weisberg, J. M. & Taylor, J. H. 2003, in *Radio Pulsars*, ed. M. Bailes, D. J. Nice, & S.E. Thorsett, (San Francisco: Astronomical Society of the Pacific), 93
- Wex, N. 1998, *MNRAS*, 298, 67